ZIBELINE INTERNATIONAL PUBLISHING

ISSN: 2521-0920 (Print)
ISSN: 2521-0602 (Online)
CODEN: MJGAAN

Malaysian Journal of Geosciences (MJG)

DOI: http://doi.org/10.26480/mjg.01.2020.38.42

RESEARCH ARTICLE

SEISMO - IONOSPHERIC INDUCED PERTURBATIONS PRIOR TO THE SEPTEMBER 28, 2007 M7.5 NORTHERN MARIANA U.S.A. GEOQUAKE FROM GPS, TEC AND DEMETER DATA

Jewel E. Thomas

Geophysics Research Group, Department of Physics, Akwa Ibom State University, Ikot Akpaden, Mkpat Enin, Akwa Ibom State, Nigeria.
****Corresponding Author Email: jewelemem@gmail.com***

ARTICLE DETAILS

Article History:

Received 10 June 2020
Accepted 14 July 2020
Available online 24 July 2020

ABSTRACT

Data from DEMETER (IAP and ISL sensors) and GPS (TEC), were used to decipher variations of electron density, electron temperature and ion density within the seismogenic zone of a seismic event that occurred on September 28, 2007 at Northern Mariana U.S.A, through statistical analysis. The study revealed both pre and post ionospheric perturbations from both sets of data. The observed anomalous variations were screened for false alarm using the geomagnetic indices of kp and Dst. It was observed that the abnormal TEC on -10, -7, -3 and -2 days occurred under quiet geomagnetic conditions while all pre-seismic (-15, -10, - 9 -7 days) ionospheric variations from the DEMETER data were also obtained during quiet geomagnetic conditions suggesting them to be seismo-ionospheric induced perturbations. Interestingly, the perturbations on -10 and -7 days were simultaneously observed from both GPS and DEMETER datasets under quiet geomagnetic ionospheric conditions offering a strong pointer to the impending geo-quake.

KEYWORDS

Geomagnetic indices, Seismogenic zones, and ionospheric perturbations.

1. INTRODUCTION

On September 28, 2007, a magnitude 7.5 geo-quake occurred in Northwest of Farallon de Pajaros, Northern Mariana Islands which is south of Japan resulting from oblique reverse faulting at intermediate depth nearly 260 km below the North Pacific Ocean and almost 300 km west of the Mariana Trench, marking where the Pacific plate begins its subduction beneath the Philippine Sea plate. Focal mechanism solutions indicate that oblique rupture occurred on either a northwest- or east-northeast-striking, moderately dipping reverse fault. Of these two possible fault orientations, finite-fault modeling of globally recorded seismic data is more consistent with slip on the east-northeast-striking fault. At the location of the earthquake, the Pacific plate moves to the west with respect to the Philippine Sea plate at a velocity of about 40 mm/yr. The earthquake represents the release of stress resulting from the distortion of the Pacific plate at depth (Hayes et al., 2017). This was just one out of the 2270 earthquakes that occurred in 2007 and due to its depth, no damage was recorded.

Earthquake is among the natural disaster that greatly impacts the Earth's surface which has proven to be dangerous to human life and properties. As a result of the complex nature of earthquake-preparation processes, finding accurate earthquake precursors from abnormal geophysical signals is still a world-class problem. Similarly, seismic activity is one of the causes of daily ionospheric inconsistency. This is due to the fact that the coupling between the anomalous generated electric field in the earthquake preparation zone at the ground surface and the one generated in ionosphere causes the ion drift that resulted in the modification of the ionosphere formation. However, to carefully forecast the geo-quake using the ionosphere, these questions must be address. (i)Is there any change in the ionosphere due to pre-seismic event and aftermath event? (ii) Having understood that there are different mechanisms responsible for the plasma distribution in the ionospheric layers, what are the basic ionospheric drivers responsible for each stages of precursor, aftermath and during the earthquake? (iii) is there any significant on latitudinal dependence of the ionospheric precursor, during and aftermath of earthquake in the ionosphere?

There is complexity with Earthquake physics. The occurrence of geo-quake is linked with the earth's crust dynamics. Due to the acoustic driven mechanisms in the atmosphere, the origin of the waves generated at the surface of the Earth penetrates into the ionosphere, thereby triggering the redistribution of the neutral gases in the ionosphere before the earthquakes (Pulinets and Boyarchuk, 2004; Pulinets and Davidenko, 2014; Ryu et al., 2014). A lot has been widely reported on the disturbances and the underlying mechanisms that cause the seismio-ionospheric coupling activities (Ondoh, 2008; Namgaladze et al., 2009; Kuo et al., 2011). Nevertheless, the electric and geomagnetic fields, neutral winds and diffusion mechanisms, as well as the acoustic gravity wave that emanated from the lower altitude of the atmosphere, are the main drivers of low- and mid-latitude ionospheric dynamics during and after the earthquake preparation (Heelis, 2004).

Various techniques and measurements had been earlier employed in the study of seismo-ionospheric precursor but notably among them is the statistical seismo-ionospheric analysis. The ionospheric earthquake precursor has been linked through various mechanisms of the formation

Quick Response Code	Access this article online	
	Website: www.myjgeosc.com	**DOI:** 10.26480/mjg.01.2020.38.42

Cite the Article: Jewel E. Thomas (2020). Seismo - Ionospheric Induced Perturbations Prior To The September 28, 2007 M7.5 Northern Mariana U.S.A. Geoquake From Gps, Tec And Demeter Data. *Malaysian Journal of Geosciences, 4(1): 38-42.*

of the ionosphere and in the atmosphere, which are valid for different ionospheric disturbances (Parrot et al., 2016; Surkov 2015). A study reported that the onset of the irregularities in the morphology of the ionosphere is of course close to the future epicenter (7-15 days) (Parrot et al., 2016). These irregularities were brought about by gravity waves that emanated from the activation of the fault where the permeability changes and where aerosols and gas including radon can appear (Surkov, 2015). This leads to the ionization of air molecules, which are responsible for the re-modification of the ionosphere. Then, different effects can occur: growth of air temperature, formation of temperature and pressure anomalies, anomalies in Outgoing Long wave infrared Radiation (OLR), redistribution of electric charges in the Earth's atmospheric system and then in the ionosphere due to the global electric circuit and electric field irregularities in the connection action.

From the above discussion, seismic precursors are still much debatable and there was no satellite mission for the detection of EQ associated ionospheric abnormalities afore the DEMETER satellite (Parrot, 2009). DEMETER (Detection of Electromagnetic Emission Transmitted from Earthquake Region) was a micro-satellite (130 kg mass) placed on an almost polar orbit with a low altitude (710 km) providing a global coverage of active seismic regions (Cussac et al., 2006). From a study the main scientific objectives of DEMETER were the variations in the ionosphere as a result of EQ induced electromagnetic activity and anthropogenic activities (Parrot, 2009). This paper studied seismo-ionospheric anomalies from both DEMETER and GPS TEC data over the EQ preparation zone (i.e. M7.5, N, Mariana U. S. A. seismic event of September 28, 2007).

2. DATA

2.1 DEMETER data

DEMETER was a low-altitude satellite which was launched in June 2004 on a polar and circular orbit that measures electromagnetic waves and plasma parameters around the world apart from in the auroral zones. Its original elevation of ~710 km was decreased to ~660 km at the end of 2005. This was the first satellite dedicated mainly to record seismo-electromagnetic effects on the ionosphere. It had six scientific payloads. Each of them offered long-time and continuously high-quality data to allow performing meaningful statistical studies with a much larger number of recorded events in comparison with previous ones. Detailed description of the DEMETER have been given by a lot of researchers (Cussac et al., 2006; Lebreton et al., 2006; Berthelier et al., 2006; Mei and Parrot, 2013; Ibanga et al., 2017). Of the six experiments in DEMETER, only two experiments (Plasma Analyser (IAP) and Langmuir Probe (ISL)) were used in this study.

The experiment IAP recorded the ion density (total ion density being the sum of H+, He+ and O+) and seismic activities that took place during the satellite's lifetime with a 4 s time resolution. The electron density and electron temperature data used in this paper were measured by the ISL experiment of the satellite. DEMETER recorded many seismic events. Figure 1, is an example of an event as recorded by it. This relates to the geo-quake of September 28, 2007 at 13:38:57 UTC having a magnitude of 7.5 and a focal depth of 260 km. Its geographic coordinates were 22.013^{0}N and 142.668^{0}E. From the top to the bottom panels, the top panel gives the header frame that includes date, orbit number, involved institutes, date and version of quick-look creation. The second panel is the ISL sweep spectrograph with the version of the onboard and ground processing frame.

The spectrogram of the Langmuir probe measures the sweep voltage in volt and collected current in log (nA). Parameters deduced from ISL measurements (ISL current and potentials) are displayed in the third panel. To this, the version of onboard and ground processing software are given at the top right side of the panel, as well as currents and potentials (Vf – floating potentials in V, ϕs – potential in V(-ϕs is displayed) and Ie-electron current in nA (log (Ie) is displayed). The bottom panel specifies the satellite closest approach of past and future EQ epicenters that are within 2000 km from the DEMETER orbit. The *Y* -axis represents the distances *D* between the epicenters and the satellite, from 750 up to 2000 km.

The symbols are filled square for post-seismic events, filled triangle for pre-seismic events. The scale on the right represents the time interval between the EQs and the DEMETER orbit with a graduation from >30 days up to a [0–6 h] interval. The empty symbols have similar significations except that they are related to the magnetically conjugated points of the epicenters (the distance *D* is then the distance between these magnetically conjugated points of the epicenters and the satellite). The symbol sizes correspond to EQs of magnitude [5–6], [6–7], and [>7]. At 00:52:00 UTC the red triangle indicates the closest approach to the epicenter of this EQ.

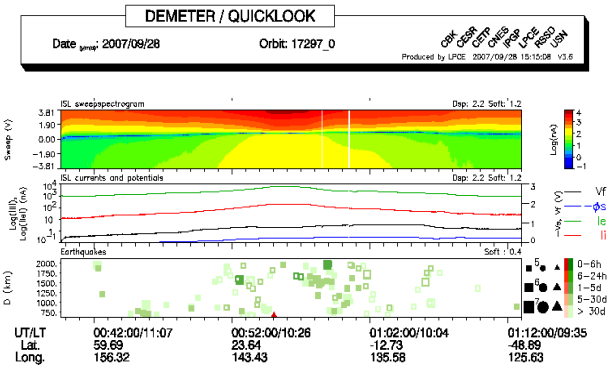

Figure 1: DEMETER orbit that recorded the anomalous variations on the earthquake day.

2.2 GPS data

The Global Positioning System (GPS) satellites are now primary sensors used to determine signatures linked with natural hazards such as earthquake. GPS is a group of satellite that orbits the earth two times per day at an elevation of about 20,000 km. The enormous network of GPS receivers (a few thousands all over the planet) elucidates simultaneous coverage in universal scale with high temporal resolution. The GPS satellites transmit two frequencies of signals (LI = 1575.42 MHz and L2 = 1227.60 MHz). These GPS receivers are able to detect ionospheric TEC perturbations caused by surface-generated Rayleigh, acoustic and gravity waves. TEC can be used to estimate spatial sizes and temporal dynamics of pre-earthquake ionospheric effects in any seismogenic region. From a list of International Global navigation satellite system service (IGS) station code, the IGS station within the radius of the earthquake preparation zone (1678.80 km) at GUUG was selected.

Request was made for the observation file within the studied time frame. Applying the RINEX Gopi software, total electron content (TEC) was calculated from the observation data. TEC variations are often explored for seismo- ionospheric precursors due to TEC data global analysis, continuous observation and satisfactory time- and space resolution plus enormous amount of the data available. This method has been used to classify variations from geo-quake (Calais and Minster, 1995). A group researchers have used a statistical approach with TEC data from TOPEX – POSEIDON to investigate connections between ionospheric perturbations and seismic event (Zaslavski et al., 1998). In other study, researchers equally used a statistical technique to obtain the ionospheric TEC from data measured by a network of the GPS in Taiwan (Liu et al., 2002).

2.3 Geomagnetic data

Local but significantly large-scale fluctuations in atmospheric electricity over seismically active zones afore the seismic event are transmitted to the ionosphere by means of a large-scale electric field. From the penetration of this electric field into the ionosphere, electron concentration irregularities are detected when the region affected has an area with a diameter larger than 200 km^2 (Dobrovolsky et al., 1979). Nevertheless, the disparities in the ionospheric strictures are not only from earthquakes as there are numerous possibilities of ionospheric distresses that can originate from other sources such as solar activity, acoustic gravity waves, traveling ionospheric disturbances, plasma dynamics, and large meteorological phenomena etc. Subsequently, the detected parameters may exhibit variations in the absence of seismic activity; hence, it is hard to segregate pre-seismic ionospheric phenomena from the ionospheric turbulences due to the solar-terrestrial activities (Ondoh, 2008).

Thus, to differentiate the seismo-ionospheric perturbations from geomagnetic instabilities, the geomagnetic indices Dst and Kp were checked. The Kp index monitors the planetary activity on a universal scale while the Dst index registers the equatorial ring current variations (Mayaud, 1980). The ionospheric influence of a geomagnetic storm has a global effect being observed all over the world while, the seismogenic impact is observed only by places with distance less than 2000 km from the potential epicenter (Pulinets et al., 2003). Data of Dst and Kp are used

to estimate the effects of geomagnetic activity. Dst data with time resolution of 1 hour are used to describe the geomagnetic activity in the middle and low latitude region. Moderate magnetic storm occurs when the Dst values are less than −50 nT while great geomagnetic storm occurs when the Dst data surpass −100 nT (Xinzhi et al., 2014). Kp data with time resolution of 3 hours indicate the global geomagnetic activity. Kp value spans from 0 (low activity) to 9 (strong activity). Kp index is less than 3 when the geomagnetic activity is quiet (Rostoker, 1972).

3. Material and Method

The M7.5 North Mariana earthquake of September 28, 2007 at an epicenter of 22.013^{0}N and 142.668 ^{0}E by 13:38: 57 UTC (11:38:57 LT) at a focal depth of 260km was selected for this study. Orbits closet to the epicenter (at a resolution of 20^0 for longitude and 10^0 for latitude) were selected 30 days prior and 10 days post the geo-quake. This time period allowed enough time to carefully monitor the ionospheric plasma parameter from its unperturbed to perturb state enhancing separation of seismic anomalies from the background of natural variations, with the expectation of the former to appear at the end of the period. Different time intervals such as two months to five days have been chosen to monitor the ionosphere but principally, reports on seismo-electromagnetic variations are observed three weeks or less to the earthquake day (Píša et al., 2011; Rong et al., 2008; Parrot, and Li, 2012).

The total ion density (Oxygen, Hydrogen and Helium ions from the IAP Sensor), electron density and electron temperature (from the ISL Sensor) were obtained by downloading data files from the DEMETER website. Data from each orbit were available in two modes (survey and burst modes) but only the burst mode data was utilized in this research. The middle and the inter-quartile range of the data were employed to find their upper and lower limits in order to differentiate seismic variances from the background of regular variations. A reference value k was selected to be 2.1. Any perturbations outside these bounds were anomalous. These involved computation of upper and lower boundaries, median value and inter-quartile range using Eqs. (1) – (3) below:

$$x_{high} = M + k \bullet IQR \tag{1}$$

$$x_{low} = M - k \bullet IQR \tag{2}$$

$$x_{low} < x < x_{high} \Rightarrow -k < \frac{x-M}{IQR} < k; Dx = \frac{x-M}{IQR} \tag{3}$$

Here x, x_{high}, x_{low}, M, IQR and Dx are parameter values, upper bound, lower bound, middle of the data, inter-quartile range and differential of x correspondingly. Thus, if the absolute value of Dx is more than k, (i.e., $|Dx| > k$) ($|Dx| > k$), then the behaviour of x is assumed to be anomalous. Similar statistical methods have been used by many researchers to isolate background perturbations from seismo- induced perturbations (Liu et al., 2004, Pulinets and Boyarchuks, 2004; Akhoondzadeh et al., 2010, Ibanga et al., 2017). However, the detected anomaly had to be crisscrossed with geomagnetic indices each day to isolate geomagnetic induced perturbations from seismo-induced variations. The radius (R) of the earthquake preparation zone was determined from Eq. (4) given (Dobrovolsky et al., 1979):

$$R = 10^{0.43M} \tag{4}$$

where M is the magnitude of the earthquake. From Eq. (4), it is obvious that the preparation zone is proportional to the geo-quake's magnitude.

4. Results

Results of DEMETER data analysis for the Mariana Island, U.S.A. earthquake (28 September, 2007) is presented in two dimensional plots (figure 2). The earthquake day (0) is represented as vertical dotted line. The lilac horizontal lines indicate the upper and lower bounds (M±2.0*IQR). The orange horizontal lines indicate the median value (M). The x-axis represents the day relative to the earthquake day. The y-axis represents (i) electron density derived from the measurements of the ISL experiment; (ii) electron temperature derived from the measurements of the ISL experiment and (iii) total ion density derived from the measurements of the IAP experiment during (a) night and (b) morning. TEC anomaly plot obtained when |DTEC| > 3, Kp < 3 and Dst > −20 (nT). is presented in figure 3. The TEC anomaly is represented as a function of the Universal Time Coordinate (UTC) and number of days relative to the main shock. Correspondingly, the contour plots of kp and Dst geomagnetic indices are shown in figure 4a and 4b. All detected anomalies from the three datasets are clearly shown in Table 1.

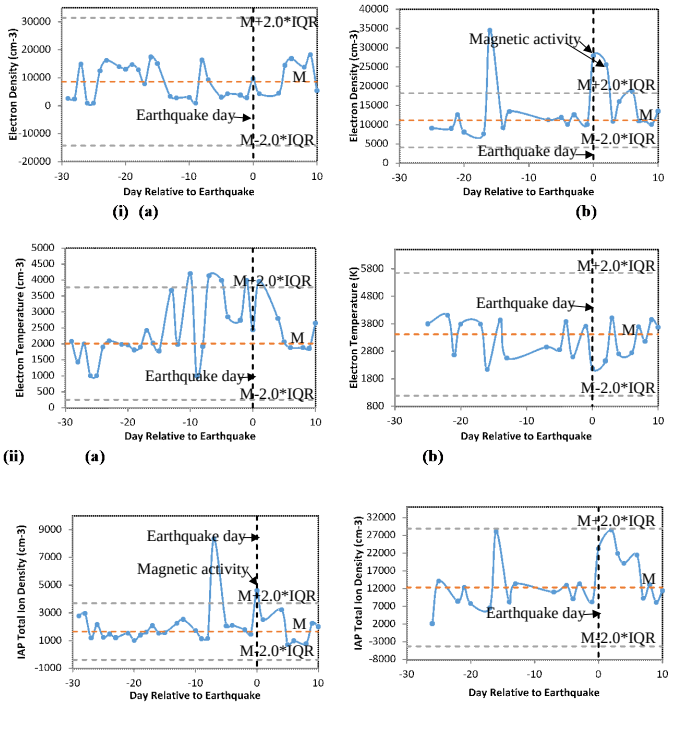

Figure 2: Results of DEMETER data analysis for the Mariana Island, U.S.A. earthquake (28 September, 2007).

The earthquake day is represented as vertical dotted line. The green horizontal lines indicate the upper and lower bounds (M±2.0*IQR). The red horizontal line indicates the median value (M).The x-axis represents the day relative to the earthquake day. The y-axis represents (i) electron density derived from the measurements of the ISL experiment; (ii) electron temperature derived from the measurements of the ISL experiment and (iii) total ion density derived from the measurements of the IAP experiment during (a) night and (b) morning.

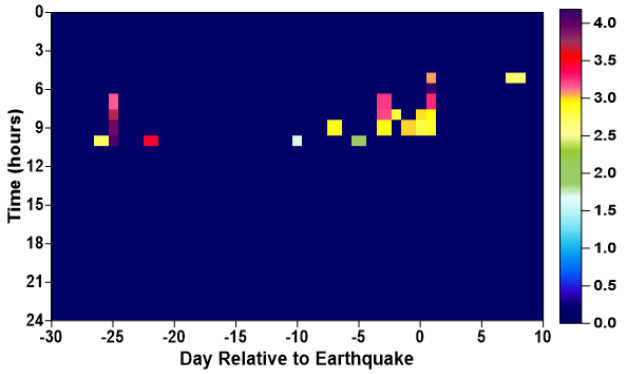

Figure 3: TEC anomaly plot detected based on: |DTEC| > 3, Kp < 3and Dst > −20 (nT).

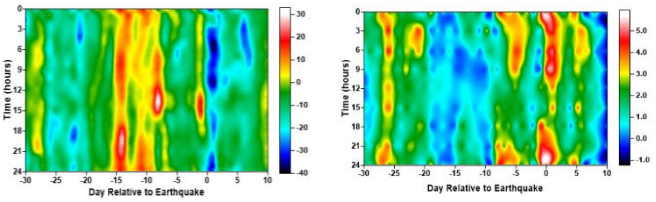

(a) kp index (b)Dst index

Figure 4: Results of analysis of variations of kp (a) and Dst (b) geomagnetic indices respectively. The y-axis represents the Time (UTC) while the x-axis represents day relative to earthquake.

Table 1: A table showing detected anomalies from all dataset. Days are relative to EQ (Day 0)

				TEC			DEMETER				GEOMAGNETIC INDICES	
Name	Date	Time	Day	Time	Value	Day	Value	Sensor	Parameter	Time	Kp	Dst
Mariana Islands region, U.S.A.	28/9/07	13:38	-26	10.00	2.56	-15	6.65	ISL	Electron density	10:30	-26	-26
			-25	7:00	3.15	-10	2.24	ISL	Electron temperature	10:30	-25	-22
			-25	8:00	3.93	-9	1.51	ISL	Electron temperature	10:30	-8	-21
			-25	9:00	4.24	-7	6.56	IAP	Total ion density	22:30	-6	-14
			-25	10.00	4.43	0	2.9	IAP	Electron density	22:30	-5	-8
			-22	10.00	3.57	0	4.79	ISL	Total ion density	10:30	-1	1
			-10	9:00	2.5	2	4.13	ISL	Electron density	10:30	0	2
			-7	9:00	2.8	6	2.15	ISL	Electron density		1	6
			-5	9:00	2.96						2	
			-3	7:00	3.26						5	
			-3	8:00	3.21						6	
			-3	9:00	2.81							
			-2	8:00	2.68							
			-1	9:00	2.94							
			0	8:00	2.91							
			0	9:00	2.66							
			1	5:00	3.02							
			1	6:00	4.58							
			1	7:00	3.31							
			1	8:00	2.82							
			1	9:00	2.73							
			8	5:00	2.53							

5. Discussion

Seismo-ionospheric induced perturbations have been widely studied using GPS and DEMETER data. In order to differentiate geomagnetic variations from seismogenic sources, the Dst and kp geomagnetic indices were checked alongside with the studied data. From the GPS data where the TEC was derived, a total of 22 anomalies were detected from 12 days (Table 1). These anomalous TEC were criss- crossed with both Dst and kp geomagnetic indices on each day. From the result, it was revealed that these geomagnetic indices were active on -26, -25, -22, -5, -1, 0, +1 and +8 days. However, the perturbations on -10, -7, and 3 and -2 days prior to the seismic event happened in quiet geomagnetic conditions. The TEC anomaly plot obtained when |DTEC| > 3, Kp < 3 and Dst > −20 (nT) (Figure 3) displayed these variations, Similarly, DEMETER data displayed 8 unusual variations from 7days.

The three investigated ionospheric plasma parameters (total ion density, electron density and temperature) were all perturbed within the studied period. On -15days, the electron density from ISL device unveiled a conspicuously high value of 6.65 in the morning orbit (Figure 2i (b)). Correlating this result with figures 4a and 4b and by virtual inspection, it is clearly seen that there was no geomagnetic activity from both indices. From the same ISL sensor, the electron temperature was perturbed on -10 and -9 days (figure 2ii (a)) with values of 2.24 and 1.50 in quiet geomagnetic conditions as portrayed by fig 4a and 4b. The IAP sensor that recorded the total ion density revealed a striking abnormal variation in the night time orbit measurement 7 days afore (figure 2iii (a)) the geo-quake having a numerical value of 6.56.

This is consistent with the reports which showed that the efficiency of the anomalous electric field penetration into the ionosphere at night is higher than in daytime Cross checking this with geomagnetic indices of kp and Dst (figure 4a and 4b), it was observed that this perturbation occurred in geomagnetically quiet conditions (Pulinets and Boyarchuk, 2004; Ibanga et al., 2017). However, the investigation revealed that the perturbations on the earthquake day (0) and after the seismic event (+2 and +6 days) (figure 2i (b) happened in active geomagnetic conditions (fig 4a and 4b). A correlation of the anomalies from both GPS and DEMETER revealed that both data sets were simultaneously disturbed on -10 and -7 days before the September 28, 2007 earthquake under quiet geomagnetic conditions. This is agreement with the reports of Parrot et al. (2016) that the onset of the irregularities in the morphology of the ionosphere is of course close to the future epicenter (7-15 days).

6. Conclusion

Seismo ionospheric induced perturbations prior to the September 28, 2007 M7.5 Northern Mariana U.S.A. Geo-quake from GPS TEC and DEMETER data have been investigated. The study revealed both pre and post (from -26 days to 6 days) ionospheric perturbations from GPS and DEMETER data. The observed anomalous variations were screened for false alarm using the geomagnetic indices of kp and Dst. The abnormal TEC on -10, -7, -3 and -2 days occurred under quiet geomagnetic conditions. All pre-seismic ionospheric variations from the DEMETER data were obtained in quiet geomagnetic conditions. Interestingly, the perturbations on -10 and -7 days were simultaneously observed in both GPS and DEMETER datasets under quiet geomagnetic ionospheric conditions. This result is in agreement with that reported by many researchers reported that the onset of the irregularities in the morphology of the ionosphere is of course close to the future epicenter (7-15 days). Nevertheless, it is important to note that the ionosphere displays complex behaviour even under quiet geomagnetic condition and the measured parameters may sometimes display variations in quiet seismic condition that can be associated with other unknown factors. The seismo ionospheric anomalies reported in this paper novel are promising for the short-term prediction. However, for further studies, attention has to be paid to further investigation leading to a very precise regional model of quiet time for ionosphere to classify seismic precursors from the background of daily variations.

Acknowledgements

The author is very grateful to the IGS community for providing the GIM-TEC data, the USGS, and Kyoto University for providing EQ details and geomagnetic storm data, respectively. Further thanks to the administration of DEMETER satellite for open access data.

References

Akhoondzadeh, M., Parrot, M., Saradjian, M.R., 2010. Electron and ion density variations and before strong earthquakes (M>6.0) using DEMETER and GPS data. Natural Hazards Earth System Sciences, 10, Pp. 7-18.

Berthelier, J.J., Godefroy, M., Leblanc, F., Seran, E., Peschard, D., Gilbert, P., Artru, J., 2006. IAP, the thermal plasma analyzer on DEMETER. Planetary and Space Science, 54, Pp. 487–501.

Calais, E., Minster, J.B., 1995. GPS detection of ionospheric perturbations following the January 17, 1994, Northridge earthquake. Geophysical Research Letters, 22, Pp. 1045–1048.

Cussac, T., Clair, M., Ultre´-Guerard, P., Buisson, F., Lassalle-Balier, G., Ledu, M., Elisabelar, C., Passot, X., Rey, N., 2006. The Demeter microsatellite and ground segment. Planetary and Space Science, 54, Pp. 413–427.

Dobrovolsky, I.R., Zubkov, S.I., Myachkin, V. I., 1979. Estimation of the size of earthquake preparation zones. Pure Applied Geophysics, 117, Pp. 1025–1044.

Hayes, G.P., Myers, E.K., Dewey, J.W., Briggs, R.W., Earle, P.S. Benz, H.M., Smoczyk, G,M., Flamme, H.E., Barnhart, W.D., Gold, R.D., Furlong, K.P., 2017. Tectonic summaries of magnitude 7 and greater earthquakes from 2000 to 2015: U.S. Geological Survey

Heelis, R.A., 2004. Electrodynamics in the low and middle latitude ionosphere: A tutorial. J. Atmos. Sol. Terr. Phys., 66, Pp. 825–838, doi: 10.1016/j.jastp.2004.01.034.

Ibanga, J.I., Akpan, A.E., George, N.J., Ekanem, A.M., George, A.M., 2017. Unusual ionospheric variations before the strong Auckland Islands, New Zealand earthquake of 30th September, 2007. NRIAG Journal of Astronomy and Geophysics, https://doi.org/10.1016/j.nrjag.2017.12.007

Kuo, C.L., Huba, J.D., Joyce, G., Lee, L.C., 2011. Ionosphere plasma bubbles and density variations induced by pre-earthquake rock currents and associated surface charges. J Geophys. Res.: Space Phys., Pp. 116. https://doi.org/10.1029/ 2011JA016628

Lebreton, J.P., Stverak, S., Travnicek, P., Maksimovic, M., Klinge, D., Merikallio, S., Lagoutte, D., Poirier, B., Kozacek, Z., Salaquarda, M., 2006. The ISL Langmuir Probe experiment and its data processing onboard DEMETER: scientific objectives, description and first results. Planet. Space Sci., 54 (5), Pp. 472–486.

Liu, J.Y., Chuo, Y.J., Pulinets, S.A., Tsai, H.F., Zeng, X., 2002. A study on the TEC perturbations prior to the Rei-Li, Chi-Chi and Chai-Yi earthquakes, In "Seismo- Electromagnetics: lithosphere-Atmosphere-Ionosphere Coupling", Eds Hayakawa, M. and Molchanov O.A., Terra Scientific Publishing Company, Tokyo, Pp. 297-301.

Liu, J.Y., Chuo, Y.J., Shan, S.J., Tsai, Y.B., Chen, Y.I., Pulinets, S.A., Yu, S.B., 2004. Pre-earthquake ionospheric anomalies registered by continuous GPS TEC measurements, Ann. Geophys., 22, Pp. 1585–1593. http://www.anngeophys.net/22/1585/2004

Mayaud, P.N., 1980. Derivation, Meaning and use of geomagnetic indices, Geophysical Monograph 22, American Geological Union, Washington DC.

Mei, L., Parrot, M., 2013. Statistical Analysis of an ionospheric parameter as a base for earthquake prediction. Journal of Geophysical Research (Space Physics), 118 (6), Pp. 3731-3739.

Namgaladze, A.A., Klimenko, M.V., Klimenko, V.V., Zakharenkova, I.E., 2009. Physical mechanism and mathematical simulation of ionosphere earthquake precursors observed in total electron content. Geomagnetism and Aeronomy, 49, Pp. 252–262.

Ondoh, T., 2008. Investigation of precursory phenomena in the ionosphere, atmosphere and groundwater before large earthquakes of M >6.5. Advance Space Research, 43, Pp. 214–223.

Parrot, M., 2009. Anomalous seismic phenomena: view from space. In: Hayakawa, M. (Ed.), Electromagnetic Phenomena Associated with Earthquakes. Transworld Research Network, Kerala, Pp. 205–233.

Parrot, M., Li, M., 2012. The use of an ionospheric parameter for earthquake prediction,paper NH44A-04, AGU Fall Meeting, San-Francisco, 3-7 December, Ionosphere Coupling. Advances in Space Research, 26 (8), Pp. 1209–1218.

Parrot, M., Tramadol, V., Liu, T.J.Y., Pulinets, S., Ouzounov, D., Genzno, N., Lisi, M., Hattori, K., Namgaladze, A., 2016. Atmospheric and Ionospheric coupling phenomena related to large earthquakes. Natural Hazards and Earth System Sciences https://doi.org/10.5194/nhess-2016-172

Píša, D., Parrot, M., Santolík, O., 2011. Ionospheric density variations recorded before the 2010 Mw 8.8 earthquake in Chile. Journal of Geophysical Research, 116, Pp. A08309; doi:10.1029/2011JA016611

Pulinents, S., Boyarchuk, K., 2004. Ionospheric precursor of earthquakes. Springer Berlin Heidelberg New York, ISBN: 3-540-20839-9.

Pulinets, S., Davidenko, D., 2014. Ionospheric precursors of earthquakes and Global Electric Circuit, Advances in Space Research doi: http://dx.doi.org/10.1016/j.asr.2013.12.035

Pulinets, S.A., Legen, A.D., Gaivoronskaya, T.V., Depuev, V.K., 2003. Main phenomenological features of ionospheric precursors of strong earthquakes. Journal of Atmospheric Solar and Terrestrial Physics, 65, Pp. 1337–1347.

Rong, Z., Feng, J., Xin-yan, O., 2008. Ionospheric perturbations before Pu'er earthquake observed on DEMETER. Acta Seismologica Sinica, 21 (1), Pp. 77 -81.

Rostoker, G., 1972. Geomagnetic Indices. Reviews of Geophysics and Space Physics, 10 (4), Pp. 935-950.

Ryu, K., Lee, E., Chae, J.S., Parrot, M., Pulinets, S., 2014. Seismo-ionospheric coupling appearing as equatorial electron density enhancements observed via DEMETER electron density measurements, J. Geophys. Res. Space Physics, 119, Pp. 8524–8542. doi:10.1002/2014JA020284

Surkov, V.V., 2015. Pre- Seismic variations of atmospheric radon activityas a possible reason for abnormal atmospheric effects, Ann. Geophysics, 58 (5), Pp. A05554.

Xinzshi, W., Junhui, J., Dongjie, Y., Fuyang, K., 2014. Analysis of Ionospheric VTEC disturbances before and after the Yutian Ms 7.3 earthquake in Xinjiang Uygur Autonomous Region. Geodesy and Geodynamics, 5 (3), Pp. 8 – 15.

Zaslavski, Y., Parrot, M., Blanc, E., 1998. Analysis of TEC measurements above active seismic regions. Physics of the earth and Planetary Interiors, 105, Pp. 219-228.